VOLUME 97 NUMBER 5

THE JOURNAL OF GEOLOGY

September 1989

UPPER MANTLE OXYGEN FUGACITY AND ITS RELATIONSHIP TO METASOMATISM[1]

GLEN S. MATTIOLI, MICHAEL B. BAKER, MICHAEL J. RUTTER, AND EDWARD M. STOLPER
Division of Geological and Planetary Sciences, California Institute of Technology, Pasadena, California 91125

ABSTRACT

We have calculated fO_2's and temperatures of various mantle environments worldwide using published analyses of coexisting olivine, orthopyroxene, clinopyroxene, and Fe^{3+}-bearing spinel from 280 peridotites. Most calculated fO_2's fall within ± 2 log units of the Fayalite-Magnetite-Quartz (FMQ) buffer at 15 kbar. Our data set defines a general trend in fO_2-T space that is not related to FMQ or to other Fe-bearing buffers. Variations in major-element, trace-element, and oxygen isotopic composition of xenoliths correlate with variations in calculated fO_2. Rare "fertile" xenoliths record fO_2's close to WM (Wüstite-Magnetite) buffer at 15 kbar and 900°C. Xenoliths with both cryptic and/or modal metasomatic overprinting are generally oxidized relative to xenoliths without evidence of such open system processing. Based on trace element and oxygen isotopic data, the best candidate for the metasomatic agent is a CO_2-H_2O-rich fluid. We suggest that metasomatic fluids are derived from oxidized, hydrated material subducted at convergent margins and that this process may have led to progressive oxidation of the earth's upper mantle through much of geologic time. This is consistent with the observation that xenoliths from Hawaii and Tahiti record fO_2's higher than mantle array's average, as do some xenoliths from the circumpacific region.

INTRODUCTION

The oxygen fugacity (fO_2) of the upper mantle has long been of interest to petrologists because of its importance both as a record of and a factor in mantle differentiation and evolution (see Arculus 1985; Mattioli and Wood 1986; Arculus and Delano 1987; and Ulmer et al. 1987 for recent reviews). Heterogeneities in the chemical potential of oxygen (or, equivalently, the fO_2) in the mantle are thought to reflect igneous and metamorphic processes that have probably been active over much of earth history. One of the most important of these processes may be mixing of recycled material at convergent margins into the mantle. Since conditions in the earth's atmosphere and oceans are far more oxidizing than those typically encountered in its interior, this mixing would generate heterogeneities, and possibly a long-term increase, in the oxidation state of multivalent cations and the fO_2's recorded by mantle rocks.

Quantitative estimates of the oxygen fugacities recorded by mantle rocks are based mostly on measurements of the ferric (Fe^{3+}) and ferrous (Fe^{2+}) iron contents of typically minor and generally Fe^{3+}-poor minerals. Because of the difficulties in obtaining accurate measurements of Fe^{3+}/Fe^{2+} ratios in these phases and because of inadequate characterizations of their thermodynamic properties, there have been until recently few quantitative determinations of the fO_2's recorded by mantle rocks and little effort to use fO_2 as a constraint on igneous and metamorphic mantle processes. Most attempts at quantitative determination of upper mantle fO_2 have had limited applicability and/or yielded potentially spurious results (see Arculus 1985; Mat-

[1] Manuscript received December 19, 1988; accepted April 25, 1989.

[JOURNAL OF GEOLOGY, 1989, vol. 97, p. 521–536]
© 1989 by The University of Chicago. All rights reserved.
0022-1376/89/9705-0007$1.00

tioli and Wood 1986; Arculus and Delano 1987; and Virgo et al. 1988 for discussion).

In this paper, we report new determinations of mantle fO_2's using published analyses of minerals from spinel-bearing peridotites brought to the surface by alkaline magmas and from ultramafic complexes. The principal difference between our work and previous efforts to quantify upper mantle fO_2 is the application of the improved thermodynamic model of Fe^{3+} in spinel and mantle rocks presented by Mattioli and Wood (1988). By examining data for suites from a range of geological environments and for some suites for which extensive geochemical data are available, we have been able to relate variations in fO_2 to other petrological and geological parameters and to infer some of the processes which lead to these variations.

SAMPLES

Our study uses published geochemical and mineral composition data. We extensively searched the literature for chemical analyses of coexisting minerals of peridotites from localities worldwide. The data sources and localities, organized into eight major geographical areas, are listed in table 1. We primarily examined data on nominally anhydrous, cryptically metasomatized (Type 1a) and some modally metasomatized (Type 1b) spinel-lherzolite and harzburgite nodules (terminology of Wilshire and Shervais 1975 as modified by Kempton 1987). These nodules are usually regarded as xenolithic fragments of upper mantle accidentally entrained in the magmas that brought them to the surface. We also examined data on 23 ultramafic-complex peridotites compositionally similar to mantle-derived nodules.

METHOD OF APPROACH

Heterogeneous Equilibrium and Thermodynamic Relations.—The fO_2's of peridotites containing olivine (ol), orthopyroxene (opx), clinopyroxene (cpx), and spinel (sp) were calculated using the following heterogeneous equilibrium:

$$2Fe_3O_4 \text{ (in sp)} + 6FeSiO_3 \text{ (in opx)} = 6Fe_2SiO_4 \text{ (in ol)} + O_2, \quad (1)$$

hereafter referred to as MFF (Magnetite [mt], Ferrosilite [fs], Fayalite [fa]). An equilibrium constant, K_1, relates the ratio of the product to reactant activities, as follows:

$$K_1(T,P) = \frac{(a^{ol}_{fa}[T,P,X])^6 fO_2}{(a^{px}_{fs}[T,P,X])^6 (a^{sp}_{mt}[T,P,X])^2} \quad (2)$$

where a^j_i is the activity of component i in phase j, T is temperature, P is pressure, and X is mole fraction. In general, each component activity in equation (2) is a function of temperature, pressure, and composition. Equation (2) can be used to calculate the fO_2 of a peridotite assemblage if K_1 and the activities of magnetite in sp, ferrosilite in opx, and fayalite in ol are known.

The equilibrium constant in equation (2) can be determined at any given T and P from the following relation:

$$\Delta H^\circ - T\Delta S^\circ = \Delta G^\circ = -RT ln K_1, \quad (3)$$

where T is in K, R is the gas constant, and ΔH°, ΔS°, and ΔG° are the standard state enthalpy, entropy, and free energy changes of equilibrium (1). The standard state enthalpy and entropy changes of equilibrium (1) were calculated by combining the phase equilibrium data of Bohlen et al. (1980) with the thermogravimetric data of Myers and Eugster (1983). These were substituted into equation (3) along with equation (2), which after rearrangement results in the following equation at 1 atm total pressure:

$$\log_{10} fO_2^{T,1\text{ atm}} = \frac{-24222}{T} + 8.64 - 6 \log_{10} a^{ol}_{fa}(T,1\text{ atm}) + 6 \log_{10} a^{opx}_{fs}(T,1\text{ atm}) + 2 \log_{10} a^{sp}_{mt}(T,1\text{ atm}). \quad (4)$$

The 1 atm $\log_{10} fO_2$'s obtained from equation (4) were corrected to the equilibration pressure (assumed to be 15 kbar) using the following relation:

$$\log_{10} fO_2^{T,P} = \log_{10} fO_2^{T,1\text{ atm}} - \frac{1}{2.303\,RT} \int_1^P \Delta \bar{V}_1 dP, \quad (5)$$

where the partial molar volume change, $\Delta \bar{V}_1$, depends on the compositions of the coexist-

TABLE 1

SAMPLE LOCALITIES

Area	Location	Reference
1) Alaska and western Canada	Seward Peninsula, Alaska	Swanson et al. 1987
	Alligator Lake, Yukon	Francis 1987
	Atlin Lake, British Columbia	Nicholls et al. 1982
	Itcha Mountains, British Columbia	
	Jacques Lake, British Columbia	Littlejohn and Greenwood 1974
	Castle Rock, British Columbia	
	Summit Lake, British Columbia	Brearly et al. 1984
2) western U.S., Central and South America	southwestern Oregon	Medaris 1977
	Kilbourne Hole, New Mexico	Kyser et al. 1981
		Bussod 1983
		Hervig and Smith 1982
	Potrillo Maar, New Mexico	Hervig and Smith 1982
	Serra Guadelupe, New Mexico	
	San Carlos, Arizona	Frey and Prinz 1978
		Hervig and Smith 1982
		Adams pers. comm. 1986
	San Quintin, Baja California	Basu and MacGregor 1975
		Kyser et al. 1981
	Sonora, Mexico	Gutmann 1986
	Rio Grande and Paraiba, Brazil	Sial 1977
	Asuncion, Paraguay	Meyer and Svisero 1987
	Patagonia, Chile	Skewes and Stern 1979
3) Pacific Ocean Islands	Tahiti	Tracy 1980
	Oahu, Hawaii	Kyser et al. 1981
		Sen 1988
4) Australia and New Zealand	Moeraki River, New Zealand	Reay and Sipiera 1987
	Kakanui, New Zealand	
	Flat Hill, Otago, New Zealand	
	Oberon, New South Wales, Australia	Morris 1986
	Victoria, Australia	Frey and Green 1974
	Tasmania, Australia	Varne 1977
5) Japan	Itinome-gata, Oga peninsula	Aoki and Shiba 1973, 1974
		Aoki and Prinz 1974
		Takahashi 1980
	Sannomegata, Oga peninsula	Arai and Saeki 1980
	Kurose, southwestern Japan	Arai and Hirai 1983
	Noyamadake, southwestern Japan	
	Miyamori ophiolite complex	Ozawa 1988
6) Asia	Tariat Depression, Mongolia	Press et al. 1986
	Mingxi, eastern China	Cao and Zhu 1987
7) Europe	Sardinia	Rutter 1985, 1987
		Albuquerque et al. 1977
	Predazzo-Monzoni Complex, Italy	Morten 1987
	Veneto region, Italy	
	Dreiser Weiher, West Germany	Stosch and Seck 1980
		Sachtleben and Seck 1981
8) Middle East and northern Africa	Aritain, northeastern Jordan	Nasir and Al-Fuqha 1988
	Harrat al Kishb, Saudia Arabia	Kuo and Essene 1986
		McGuire 1988
	Zabargad Island	Bonatti et al. 1981
	Hoggar, southern Algeria	Girod et al. 1981
	Assab, Ethiopia	Piccardo and Ottonello 1978
	Cameroon, Africa	Dautria and Girod 1987

ing phases. Molar and excess volumes used to calculate $\Delta\bar{V}_1$ are from Mattioli and Wood (1988) and are assumed to be independent of T and P.

For comparison, we also calculated MFF standard state properties from thermochemically measured enthalpies of formation and third law entropies for fs and fa (Berman and Brown 1985 as modified by Sack and Ghiorso 1989) and mt (Robie et al. 1978). This comparison allowed us to assess both the internal consistency of our formulation of MFF with the activity-composition relations we chose for $FeSiO_3$ and Fe_2SiO_4 (see discussion below) and to estimate the uncertainty attributable solely to the standard state data. At 850°C and 1 atm, the two data sets yield values of lnK_1 that agree within 0.37.

Activity Coefficients.—We have chosen a pure phase standard state at the T and P of interest for the current calculations; *i.e.*, for all T and P, the individual activities of Fe_3O_4 (mt), $FeSiO_3$ (fs), and Fe_2SiO_4 (fa) are equal to unity when their mole fractions in sp, opx, and ol, respectively, are unity. In natural peridotite assemblages, however, the concentrations of mt, fs, and fa are low (*i.e.*, $a_i^j \ll 1$). Accordingly, we require activity-composition relations at 1 atm for mt, fs, and fa components in sp, opx, and ol in order to calculate fO_2's from equation (4). For all phases, the effect of pressure on activity is included in the excess volume term of equation (5).

Spinel: The experimental calibration of Mattioli and Wood (1988) was used to calculate magnetite activities in complex $MgAl_2O_4$-Fe_3O_4-$FeCr_2O_4$-$FeAl_2O_4$ spinels. Ryabchikov et al. (1986) and O'Neill and Wall (1987) also present models for magnetite activity that they applied to spinel-bearing assemblages to estimate upper mantle fO_2's. We have chosen the Mattioli and Wood (1988) formulation because it is the only one that has been calibrated over much of the temperature and composition range relevant to spinels from mantle xenoliths and also includes the effects of ordering along the $MgAl_2O_4$-Fe_3O_4 join. The Mattioli and Wood (1988) formulation, moreover, is easier to apply to natural assemblages than that of O'Neill and Wall (1987) because a non-linear solution for the cation distribution in complex spinels is not necessary for each determination of fO_2.

Orthopyroxene: Natural orthopyroxenes contain up to 5.6 wt % Al_2O_3, which removes their compositions from the $FeSiO_3$-$MgSiO_3$ binary, so ferrosilite activity in Al-bearing opx was calculated using the model of Kawasaki and Matsui (1983) for Al-bearing opx. Their formulation and excess parameters for complex Al-bearing opx solid solutions are approximately equivalent to a 1-site, symmetric, regular solution model for the $FeSiO_3$-$MgSiO_3$ binary with W_G = 1.0 kcal/g-atom.

Olivine: Fayalite activity in olivine was calculated using the formalism of Davidson and Mukhopadhyay (1984) for quadrilateral olivines, although olivines in mantle xenoliths generally contain less than 1.0 wt % nonbinary components. We modified their published solution parameters to be consistent with ol-opx exchange data recently reviewed by Sack and Ghiorso (1989) in order to maintain internal consistency with ferrosilite activity-composition relations (Kawasaki and Matsui 1983) and MFF standard state data. The final excess parameters we chose for olivine are within Sack and Ghiorso's stated range, and they result in a calculated fO_2 similar to that reported by Mattioli and Wood (1988) for a simple model xenolith. The olivine model we used is approximately equivalent to a 2-site, symmetric, regular solution model for the Fe_2SiO_4-Mg_2SiO_4 binary with W_G = 1.5 kcal/g-atom.

Calculation Procedure.—Ferric iron contents of the spinels were calculated from published spinel analyses assuming R_3O_4 stoichiometry and that Fe is the only cation with variable valence. In a recent study of mantle-derived ilmenites, Virgo et al. (1988) report that Fe^{3+} contents calculated from electron probe analyses assuming stoichiometry are systematically higher than those calculated from Mössbauer spectroscopy. In contrast, a similar study on defect-poor Fe_3O_4-$MgAl_2O_4$ synthetic spinels indicates that Fe^{3+} contents calculated from electron probe analyses assuming stoichiometry are close to or slightly lower than those determined from Mössbauer spectroscopy (Mattioli et al. unpublished data). We therefore assume that R_3O_4 stoichiometry is closely approximated in most mantle-derived spinels. Iron was assumed to be entirely in the ferrous state in ol, opx, and cpx. Cation site assignments for the silicate

phases were done using conventional assumptions (Wood and Banno 1973; Gasparik and Newton 1984). The distributions of Fe^{2+} and Mg on octahedral M1 and M2 sites in ol, opx and cpx were assumed to be random.

We calculated fO_2's for 280 peridotites whose mineral compositions were obtained from the literature. For each peridotite, the procedure was first to calculate an equilibration temperature using an opx-cpx thermometer (Wood and Banno 1973 as modified by Wells 1977). Activities of fa, fs, and mt were calculated at 1 atm given the reported mineral chemistries and the activity-composition relationships for each phase discussed in the preceding section. Equations (4) and (5) were then used to calculate $\log_{10} fO_2$; the equilibration pressure was assumed to be 15 kbar for all peridotites. This procedure was then repeated for each peridotite using an equilibration temperature based on an Al-in-opx thermometer (Gasparik and Newton 1984 as modified by Webb and Wood 1986).

None of the investigations from which peridotite mineral chemistry was obtained reported direct spectroscopic or wet chemical determination of ferric iron contents in the silicate phases. Accordingly, we treated all Fe in the silicate phases as ferrous. In a parallel set of calculations, however, we explicitly calculated ferric iron contents in each silicate phase by charge and mass balance. We found that the general trend of temperature-fO_2 pairs (see below) was not significantly different using either the assumption of no ferric iron or the calculated ferric iron contents in the silicate phases.

Final Data Selection.—Most published investigations of peridotites provide little information on textures or chemical variation across grain boundaries of different phases or between edges and cores of individual grains. This makes it difficult to assess whether reported mineral compositions reflect equilibrium compositions. Moreover, some analyses may be in error or inaccurate. In order to exclude disequilibrium assemblages and inaccurate analyses, we limited our consideration to data that passed the tests described in the following paragraphs.

Consistency between thermometers: In figure 1, we plot the calculated Al-in-opx temperature against the calculated opx-cpx temperature for each peridotite in the full data

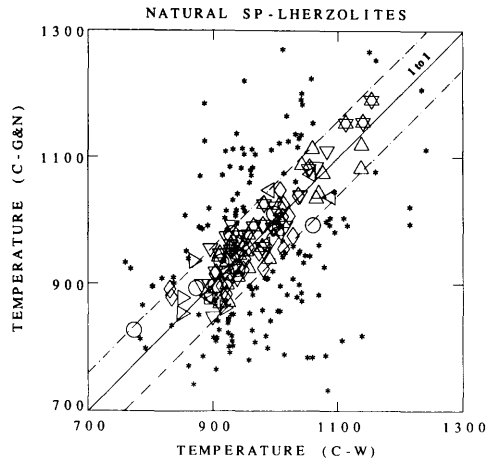

FIG. 1.—Calculated equilibration temperatures (°C) based on the opx-cpx (Wells 1977) and the Al-in-opx thermometers (Gasparik and Newton 1984 as modified by Webb and Wood 1986). Xenolith suites from the eight major geographic areas of table 1 are coded with different symbols: (1) Alaska and western Canada—upward pointing triangles; (2) Western U.S., Central and South America—diamonds; (3) Pacific Ocean Islands—downward pointing triangles; (4) Australia and New Zealand—squares; (5) Japan—rightward pointing triangles; (6) Asia—leftward pointing triangles; (7) Europe—stars; (8) Middle East and Northern Africa—circles. Perfect agreement between the two thermometers is indicated by the solid line labeled 1 to 1; ±30° test is shown by the dot-dash lines. Individual peridotites that were eliminated from the final data set as a result of "failing" the tests outlined in the text are shown as asterisks.

set. Peridotites were included in the final data set only if the two calculated equilibration temperatures overlapped within a reasonable estimate of an absolute error of ±30°C for each thermometer. This assumes that both thermometers are calibrated with similar precision over the entire range of temperature, pressure, and composition, and that they should yield equivalent temperatures. Observed deviations between the two temperatures are distributed randomly over the entire range of calculated temperatures and do not appear to be offset in any systematic way, which supports this assumption. One-hundred forty-two samples out of 280 were eliminated based on this criterion. Peridotites discarded from the final data set as a result of failing this or one of the other tests outlined below are shown in figure 1 and all subsequent figures as small asterisks. Our final data set is represented by different polygons, cor-

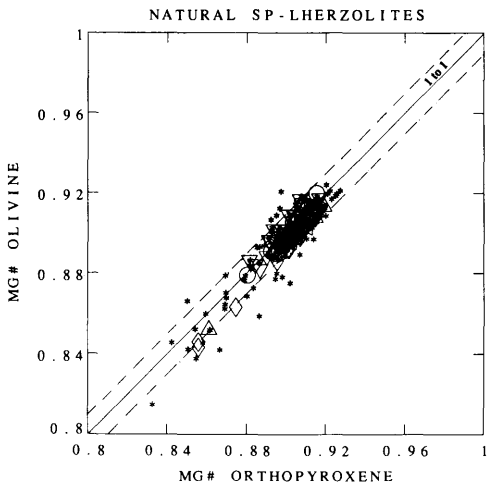

FIG. 2.—Mg# in ol versus Mg# in opx. All Fe was assumed to be Fe^{2+} in both phases. Symbols are the same as in figure 1. Perfect agreement between the two Mg#'s is indicated by the solid line labelled 1 to 1; ±0.01 test is shown by the dot-dash lines. Note the increased scatter with decreasing Mg# of both phases.

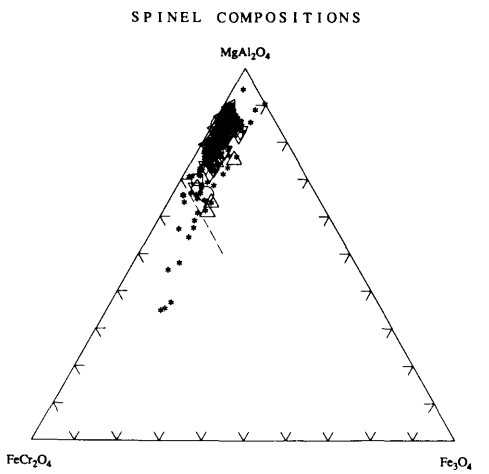

FIG. 3.—Spinel compositions projected into the system $MgAl_2O_4$-Fe_3O_4-$FeCr_2O_4$ from either $MgCr_2O_4$ or $FeAl_2O_4$. These components are generally less than 4 mole % of any natural spinel. Fe_3O_4 activities in synthetic spinels were calibrated along the Fe_3O_4-$MgAl_2O_4$ join and at two points in the ternary with X_{chrm} = 0.25 and X_{mt} = 0.04 and 0.08 by Mattioli and Wood (1988). Peridotites with spinel compositions falling below the dashed line were eliminated from the final data set. Symbols are the same as in figure 1.

responding to the eight different geographical areas listed in table 1.

Fe-Mg distribution between olivine and orthopyroxene: Further indication of major element equilibrium between phases of individual peridotites was obtained by plotting the Mg#, *i.e.*, molar [Mg/(Mg + Fe^{2+})], of one silicate phase against that of another. Such plots generally yielded tightly clustered linear arrays. In figure 2, we plot Mg# in ol against Mg# in opx. This figure demonstrates the close approximation to unit slope of the final data set, in good agreement with a new calibration of Fe-Mg partitioning between ol and opx over the temperature and composition range of peridotitic assemblages (Sack and Ghiorso 1989). Only four samples that passed the thermometer test were deleted from the final data set because their Mg# in ol and opx disagreed by more than 0.01. This test is much less discriminating than the opx-cpx vs. Al-in-opx temperature comparison. We note that the discrepancy between Mg# in ol versus Mg# in opx increases with decreasing Mg-content in both phases. The relatively Fe-rich assemblages could contain small concentrations of Fe^{3+} in the pyroxenes; if so, this could contribute to the apparent discrepancy between the two thermometers.

Suspect spinel analyses: Several peridotites were eliminated from the final data set because the calculated X_{mt}^{sp} was less than 0.006. The apparent lack of ferric iron in these samples, as determined by stoichiometry, probably is in some cases an artifact of poor electron probe standards or procedures. Only 25 of 280 peridotites were eliminated solely because of this criterion.

Spinels outside the calibrated compositional range: Other peridotites were eliminated from the final data set if their spinel compositions were well outside the range of experimental calibration of Mattioli and Wood (1988) (*i.e.*, spinels with $X_{FeCr_2O_4} + X_{FeAl_2O_4} \geq 0.3$). In figure 3, we plot the natural spinel compositions in mole % projected into the $MgAl_2O_4$-Fe_3O_4-$FeCr_2O_4$ ternary system. Only nine of 280 peridotites were eliminated because of this criterion alone; five of the nine eliminated on this basis were from the 23 peridotite samples from ultramafic complexes.

Based on these criteria (comparability of two thermometers; agreement of ol and opx Mg#; non-zero magnetite component; spinel composition in the experimentally calibrated

range), the complete data set of 280 peridotites was narrowed to 99. Although some "good" sets of analyses were probably eliminated by these filters, we doubt that many "bad" sets of analyses were allowed to pass through.

Uncertainty Estimates for Oxygen Barometry and Geothermometry.—The following are our estimates of individual errors that contribute to the uncertainty of upper mantle fO_2 calculations.

Standard state data: Uncertainties in the enthalpy and entropy of equilibrium (1) yield lnK_1 with ± 0.37 precision at 850°C and 1 atm. This corresponds to an uncertainty of ± 0.16 $\log_{10} fO_2$.

Ferric iron contents in sp: Both Bence-Albee and ZAF reductions of wavelength dispersive electron microprobe analyses yield X_{mt}^{sp} with ± 0.005 precision for X_{mt}^{sp} of 0.04 (the mean value of the final data set). This corresponds to ± 0.3 $\log_{10} fO_2$ at 900°C. The uncertainty associated with fO_2 increases with decreasing X_{mt}^{sp} and thus decreasing fO_2 at constant temperature.

Compositions of ol and opx: Uncertainties as a result of electron microprobe analyses of these phases correspond to ± 0.15 $\log_{10} fO_2$ at 900°C.

Temperature: A temperature uncertainty of ±30°C at 900°C produces an uncertainty of ± 0.5 $\log_{10} fO_2$ for an X_{mt}^{sp} of 0.04. This estimate includes the effect of temperature on the component activities and the standard state data.

Pressure: The stability field of Cr-bearing spinel-lherzolites ranges approximately from 5 (with coexisting plagioclase) to 28 kbar (with coexisting garnet) at 1100°C (Wood and Yuen 1983; Webb and Wood 1986). We assumed a uniform equilibration pressure of 15 kbar for the present calculations. An uncertainty of ±5 kbars translates into an fO_2 uncertainty of approximately ± 0.25 $\log_{10}$ units at 900°C (Mattioli et al. 1987).

We performed a Monte Carlo simulation to assess the propagation of the individual errors outlined above. In our analysis we assumed that the errors associated with each variable could be described by a gaussian distribution. The following relative errors were assigned: standard state data and equilibration temperature (3%); partial molar volume (5%); fayalite and ferrosilite activities (10%); and magnetite activity (25%). The variation in pressure was treated with a uniform distribution and varied between 10 and 20 kbars. The calculated cumulative error is less than ± 0.9 $\log_{10} fO_2$ at 1000°C and 15 kbar.

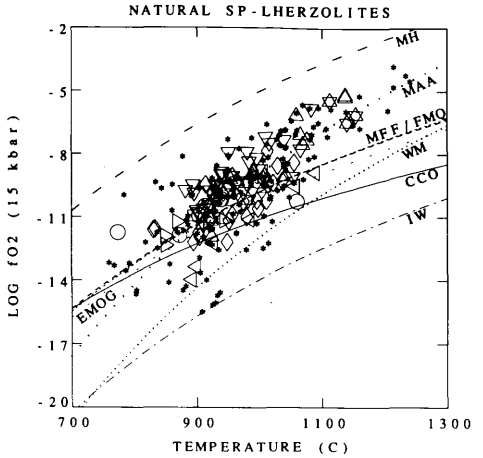

FIG. 4.—Calculated $\log_{10} fO_2$'s for the complete data set (excluding peridotites with suspect spinel analyses, *i.e.*, $X_{mt} \leq 0.006$). Temperatures are calculated from the opx-cpx thermometer and 1 atm fO_2's were corrected to 15 kbar. The following buffers are shown for reference: Iron-Wüstite, IW; Graphite-CO-CO_2, CCO; Wüstite-Magnetite, WM; Enstatite-Magnesite-Olivine-Graphite, EMOG; Magnetite-Ferrosilite-Fayalite, MFF; Fayalite-Magnetite-Quartz, FMQ; and Magnetite-Hematite, MH. Molar volume data used to correct these buffers to 15 kbar total pressure are from Robie et al. (1978). The effects of isothermal compression and isobaric expansion on the solid buffers are small and were ignored for the present calculations. Also shown as a dotted-line is our estimate of the trend of the final data set, which is referred to as the Mantle Array Average (MAA) in the text. Calculated fO_2's generally fall between WM and approximately 3 $\log_{10}$ units above FMQ and 800° and 1150°C.

RESULTS

Calculated fO_2 and opx-cpx equilibration temperatures are plotted in figure 4 and tabulated in Appendix 1, which is available from *The Journal of Geology* free of charge upon request. Also plotted are the pressure-corrected (15 kbar) iron-bearing buffers (Myers and Eugster 1983), the graphite-vapor saturation surface (Woermann and Rosenhauer 1986), and enstatite-magnesite-olivine-graphite (EMOG) buffer (Eggler and Baker 1982). Temperature-fO_2 pairs included in the final data set range between 850° and 1150°C

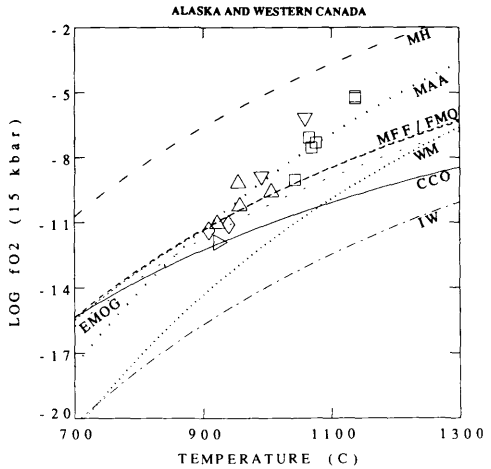

A

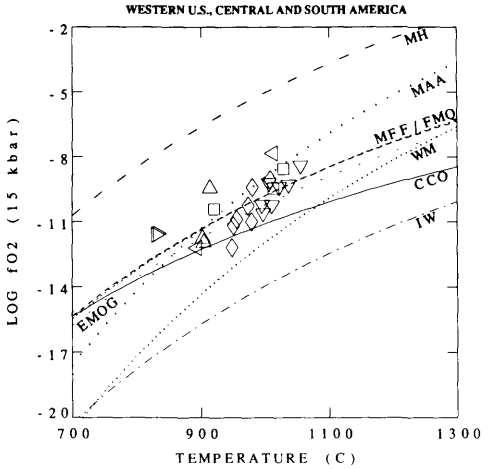

B

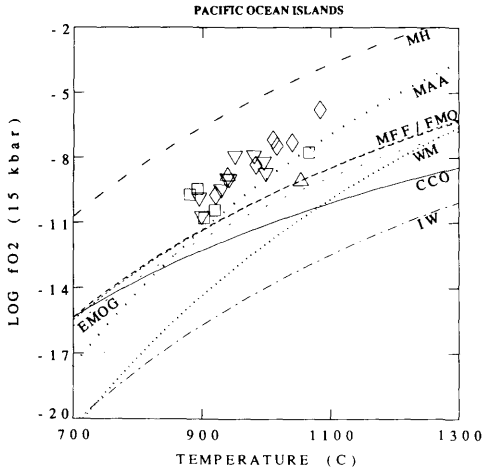

C

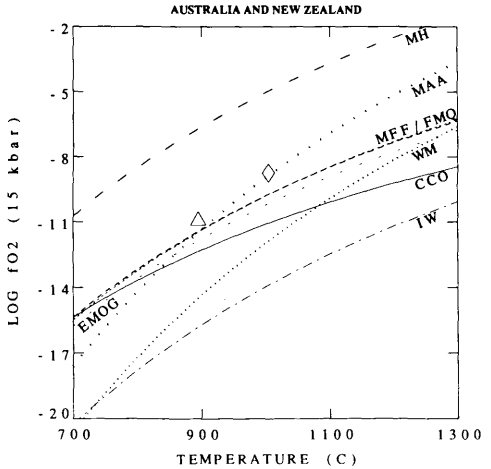

D

FIG. 5.—Calculated $\log_{10} fO_2$'s for peridotites from locations within the eight major geographic areas listed in table 1. Only peridotites in the final data set are included in figures 5*A* through 5*H*. Synthetic buffers are shown for reference and are labelled as in fig. 4. Note that individual suites generally parallel MAA and that each of the eight geographic areas apparently have much smaller ranges than the global data set. (*A*) Alaska and western Canada: Seward peninsula, Alaska—rightward pointing triangles; Alligator Lake, Yukon—upward pointing triangles; Atlin Lake, British Columbia—diamonds; Castle Rock, British Columbia—downward pointing triangles; Summit Lake and Itcha Mtns., British Columbia—squares. (*B*) Western U.S., Central and South America: Western Oregon ultramafic complex—upward pointing triangles; Kilbourne Hole, Serra Guadelupe, Potrillo Maar, New Mexico—diamonds; San Carlos, Arizona—downward pointing triangles; Sonora, Mexico—squares; Rio Grande and Paraiba, Brazil—rightward pointing triangles; Patagonia, Chile—leftward pointing triangles. (*C*) Pacific Ocean Islands: Tahiti—upward pointing triangles; Kaau, Oahu, Hawaii—diamonds; Salt Lake Crater, Oahu, Hawaii—downward pointing triangles; Kalihi, Oahu, Hawaii—squares. (*D*) Australia and New Zealand: Tasmania, Australia—upward pointing triangle; Victoria, Australia—diamond. (*E*) Japan: Ichino-megata—upward pointing triangle; Sannomegata—diamond; Ichino-megata (Takahasi data)—downward pointing triangles; Miyamori ultramafic complex—squares. (*F*) Asia: Tariat Depression, Mongolia—stars; southeastern China—circle. (*G*) Europe: Sardinia—upward pointing triangles; Venetto, Italy—diamond; Dreiser Weiher, West Germany (Amphibole-bearing xenoliths)—downward pointing triangles; Dreiser Weiher, West Germany (Anhydrous)—squares. (*H*) Middle East and Northern Africa: Zabargad Island—upward pointing triangle; Hoggar, Africa—diamonds; Cameroon, Africa—downward pointing triangle.

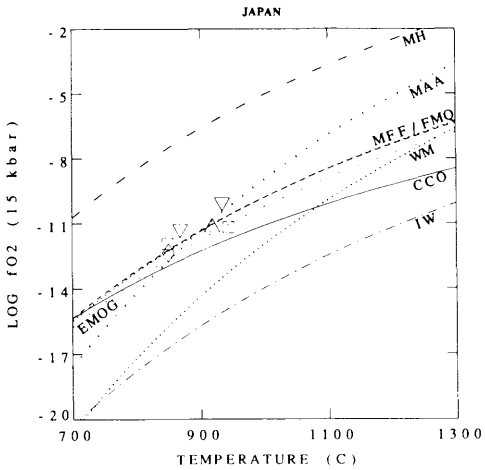

E

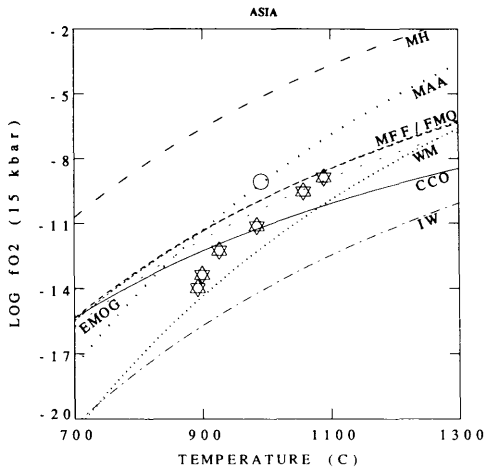

F

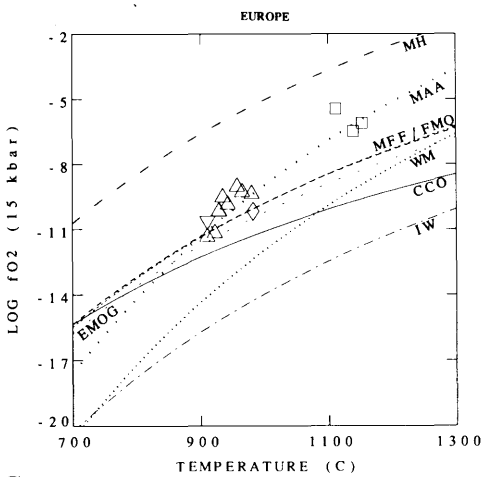

G

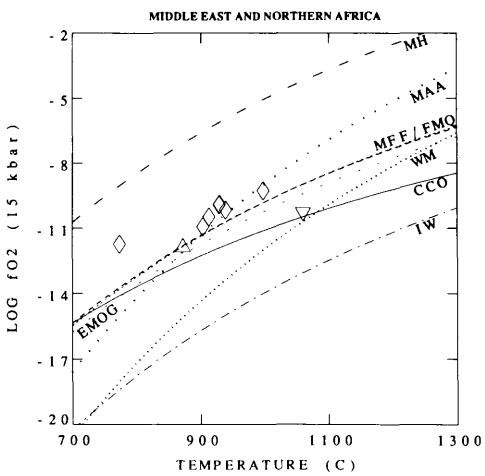

H

and -15 and -6 log units. It is clear from figure 4 that the mantle fO_2 array is not parallel to and has a steeper slope than the synthetic iron-bearing buffers (IW, FMQ, MFF, and MH) and is not approximated by either the vapor saturated graphite-CO_2 surface or EMOG. In order to facilitate intra- and intersuite comparison, we have selected a reference T-fO_2 trend labeled as MAA (mantle array average) on figure 4. MAA is parallel to WM but shifted to higher fO_2 values by 3 $\log_{10}$ units. In figures *5a* through *5h*, we have plotted individual suites in each of the eight major geographic areas listed in table 1. Inspection of these figures reveals that individual suites generally parallel MAA.

In subsequent figures and discussion, we reference the calculated fO_2 for each xenolith to MAA; *i.e.*, the $\log fO_2$ defined by MAA at any temperature was subtracted from the calculated $\log fO_2$ of each xenolith to produce a $\Delta\log fO_2$ (rock-MAA). Xenoliths that are more oxidized than the population as a whole thus have positive $\Delta\log fO_2$'s, while those that are more reduced have negative $\Delta\log fO_2$'s.

DISCUSSION

Given that equation (1) corresponds to the MFF buffer, it is somewhat surprising that the array of data (MAA) cuts across this and other iron-bearing buffers. This is not an artifact of our final data selection, since the full data set, including the discarded analyses

shown as asterisks, follows a similar trend. Part of the explanation for this trend lies in the temperature-dependence of the activity-composition relationships we have chosen. This is demonstrated by the fact that if we keep all phase compositions fixed and calculate the fO_2 at different temperatures, a trend is generated that deviates from MFF in the same direction but to a lesser extent than the actual xenoliths. We suggest that this effect is enhanced further by closed-system subsolidus reequilibration between the phases during cooling, which results in dilution of the magnetite component in spinel as the pyroxenes become less aluminous. This would tend to decrease fO_2 relative to the trend for constant mineral chemistry.

Comparison with Other Studies.—Our procedures yield fO_2's approximately 0.9 $\log_{10}$ units more oxidized than those reported by O'Neill and Wall (1987) for samples 270 and 271 of Arculus and Delano (1981). This difference reflects slightly different activity-composition relations for mt, fs, and fa and standard state data adopted by us versus those adopted by O'Neill and Wall (1987). We note, however, that both methods suggest that these xenoliths equilibrated near the fayalite-magnetite-quartz buffer at elevated pressure, not near or below the iron-wüstite buffer as indicated by the "intrinsic" fO_2 measurements of Arculus and Delano (1981). In addition, a recent investigation of discrete ilmenite-bearing nodules from kimberlites of western Africa yields $\log fO_2$'s within ± 1 log unit of FMQ over a temperature range of 600° to 1200°C (Haggerty and Tompkins 1983). This study also confirms the generally oxidized nature of the shallow upper mantle.

Comparison of the Ryabchikov et al. (1986) activity model for spinels with the Mattioli and Wood (1988) formulation indicates that all other parameters being equal, calculated fO_2's will agree to within 0.5 $\log_{10}$ units.

Relationship of Upper Mantle Oxygen Fugacity to Xenolith Chemistry.—Geochemical data are not available for ultramafic-complex-peridotites of our data set, so our discussion of the relationship of upper mantle oxygen fugacity to peridotite chemistry will be restricted to peridotite nodules found in alkali basalts. Type 1 xenoliths are generally interpreted as residues of the extraction of basic

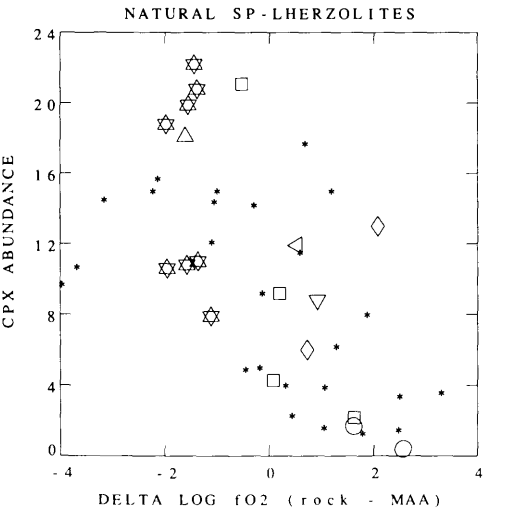

FIG. 6.—Cpx abundance versus $\Delta\log_{10} fO_2$ (rock-MAA) for selected xenoliths for which there are extensive geochemical data. Note the general inverse correlation between modal cpx content and relative oxidation. Cpx abundance was obtained either from mass balance using mineral and bulk major element chemistry or point counting grains in thin section. Locations and symbols for figures 6–10 are as follows: Kilbourne Hole, New Mexico—upward pointing triangles; Salt Lake Crater, Oahu, Hawaii—diamond; Dreiser Weiher, West Germany (Amphibole-bearing xenoliths)—downward pointing triangles; Dreiser Weiher, West Germany (Anhydrous)—squares; Sardinia—rightward pointing triangles; Victoria, Australia—leftward pointing triangles; Tariat Depression, Mongolia—stars; Assab, Ethiopia—circles. Some locations are absent from specific figures as a result of incomplete data. Xenoliths that "failed" only the temperature overlap test are shown as asterisks on this and subsequent figures.

melts from more fertile peridotites (Wilshire and Shervis 1975; Frey and Prinz 1978). Melting experiments on representative lherzolites in the spinel lherzolite stability field show the modal abundance of cpx in the residue decreases as melt fraction increases and that cpx is the first major silicate phase to be consumed (Green and Ringwood 1967; Jaques and Green 1986; Takahashi 1986). In figure 6, we plot cpx abundance versus $\Delta\log fO_2$ (rock-MAA) for xenoliths included in our study for which cpx abundance had been measured or could be estimated from major element chemistry. Although there is considerable scatter, there is an inverse correlation between cpx abundance and $\Delta\log fO_2$ which

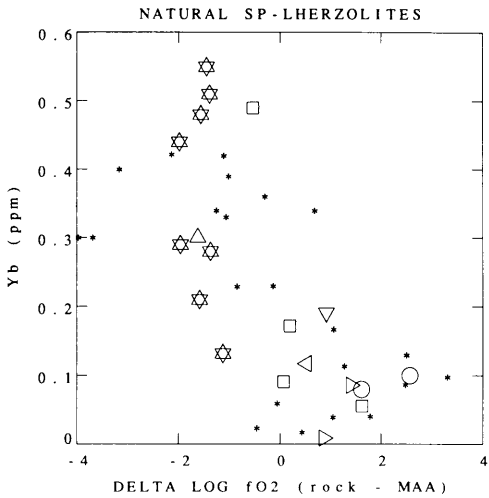

FIG. 7.—Yb (ppm) in whole rock versus $\Delta\log_{10}fO_2$ (rock-MAA). Data sources for figures 7 and 8 are: Kilbourne Hole (Roden et al. 1988); Dreiser Weiher (Stosch and Seck 1980); Sardinia (Dupuy et al. 1987); Victoria (Frey and Green 1974); Mongolia (Stosch et al. 1986); and Assab (Ottonello 1980). "Primitive" upper mantle has a bulk Yb content of 0.42 ± 0.02 (Jagoutz et al. 1979; Hart and Zindler 1986). Symbols are the same as in figure 6.

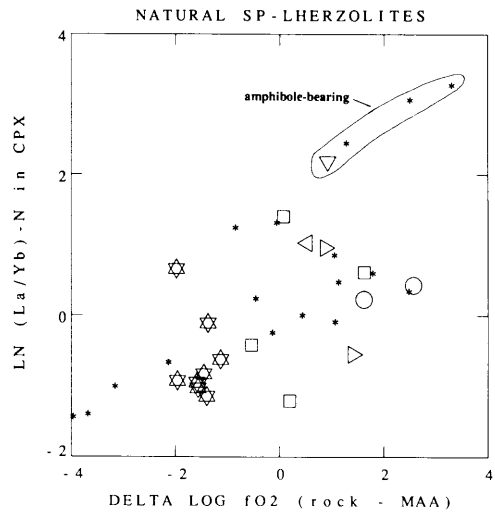

FIG. 8.—Ln (La/Yb) in cpx normalized to bulk average chondritic abundances (Boynton 1984) versus $\Delta\log_{10}fO_2$ (rock-MAA). There is a general positive correlation between relative oxidation and LREE-enrichment. The most LREE-enriched samples contain secondary volatile-rich phases. Symbols are the same as in figure 6.

implies that the most fertile xenoliths (*i.e.*, those with highest cpx abundance) are the most reduced. This is further supported by the fact that total heavy rare earth concentrations are negatively correlated with $\Delta\log fO_2$ (rock-MAA) (fig. 7).

There are many possible explanations of the inverse relationship between "fertility" and degree of oxidation. For example, although we have postulated that closed system, subsolidus heating or cooling of peridotite assemblages follow MAA in T-$\log fO_2$ space, it is possible that as peridotites begin to melt, their paths become steeper than MAA (*i.e.*, that fO_2 increases with T more strongly than along MAA); although we consider the opposite to be more likely, this could contribute to the trends in figures 6 and 7. Alternatively, partial melting could be related to the influx of oxidized, volatile-rich fluid (Lloyd and Bailey 1975), such that when more of such fluid is introduced, the degree of melting is greater and the source (and subsequent residue) is more oxidized. Another possibility is that more depleted peridotites were preferentially subject to metasomatism by oxidizing fluids (Frey and Green 1974; Frey 1983). Although it is not possible to distinguish definitively between these or other possible explanations for the observed trends in figures 6 and 7, several observations point to secondary oxidation of depleted peridotites by some open system process as the ultimate cause.

Chondrite-normalized LREE/HREE ratios are generally used to assess the presence and degree of cryptic metasomatism, with higher ratios indicating metasomatic enrichment of LREE (Frey and Green 1974; Frey 1983). We characterize LREE enrichment by a xenolith's chondrite-normalized (Boynton 1984) La/Yb ratio of separated cpx; *i.e.*, a xenolith whose chondrite-normalized (La/Yb) ratio in cpx is >1 is LREE-enriched, while a xenolith whose chondrite-normalized (La/Yb) ratio in cpx is <1 is LREE-depleted. The presence of hydrous phases is also generally regarded as evidence of an influx of some metasomatic agent into a previously anhydrous xenolith (Harte 1983; Dawson 1984). In figure 8, we plot the natural logarithm of the chondrite-normalized (La/Yb) ratio in cpx versus $\Delta\log fO_2$. Despite the scatter, there is a positive correlation between LREE-

enrichment and the degree of oxidation. In general, xenoliths with the highest (La/Yb) ratios also contain secondary hydrous phases such as pargasitic amphibole or phlogopite. One relatively oxidized sample in our data set with a relatively high (La/Yb) ratio also contains minor apatite, a feature that has been associated with metasomatism (Harte 1983). The simplest explanation of these observations, and the one that we prefer, is that preferential metasomatism of depleted peridotites led to their oxidation, increased La/Yb ratios, and in some cases produced volatile-rich phases. Progressive metasomatism leading to oxidation has been previously suggested by several authors (*e.g.*, Lloyd and Bailey 1975; Boettcher and O'Neil 1980).

The hypothesis that metasomatism of mantle rocks leads to their oxidation is strongly supported by recent detailed study of xenoliths from Tariat, Mongolia, and Eifel, West Germany (Stosch and Seck 1980; Stosch et al. 1986; Harmon et al. 1986; and Kempton et al. 1988). The xenoliths from Mongolia are some of the most fertile, least LREE-enriched, and most reduced of the xenoliths in our data set, and they contain scant evidence of secondary hydrous phase formation. In contrast, the Eifel xenolith population contains among the most oxidized samples in our data set, and some xenoliths contain secondary hydrous phases and are highly LREE-enriched. Based on comparison of similar data sets for both localities, Harmon et al. (1986) concluded that the Mongolian xenoliths primarily reflect closed system behavior in the upper mantle, while Kempton et al. (1988) showed that the West German suite has abundant evidence for open system exchange with some metasomatic agent. Strong evidence for this contrasting behavior comes from the differences between the $\delta^{18}O$ of cpx and ol [$\Delta^{18}O$ (cpx-ol)]. Open system behavior is reflected by a decrease in $\Delta^{18}O$ (cpx-ol) from initial values of 0.8 to 1.4 toward final values of -0.4. In addition, Kempton et al. (1988) found that $\Delta^{18}O$ (cpx-ol) was inversely correlated with (La/Yb) ratios in cpx. Figure 9 shows that $\Delta^{18}O$ (cpx-ol) is also inversely correlated with $\Delta\log fO_2$ (rock-MAA) for these two suites. For these two suites, there is thus an excellent correlation between LREE enrichment, modal cpx (see fig. 7), mineralogical and stable isotope evidence for

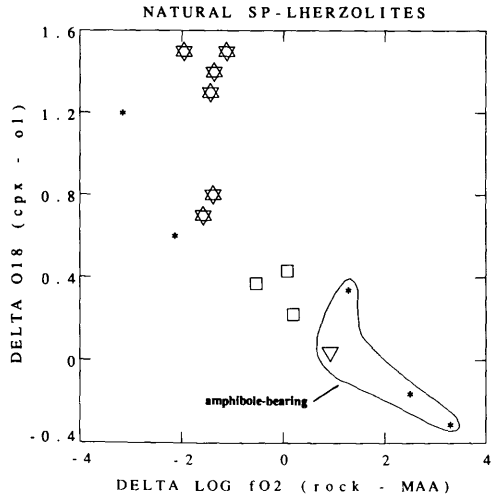

FIG. 9.—ΔO^{18} (cpx-ol) vs. $\Delta\log_{10} fO_2$ (rock-MAA). There is a correlation between the degree of oxygen isotopic disequilibrium and relative oxidation. Symbols are the same as in figure 6.

secondary metasomatism by hydrous fluid, and fO_2. Taken together, these correlations strongly support the hypothesis that secondary processes involving interaction with an oxidizing fluid generate heterogeneities in fO_2 in the upper mantle. Although there are other possibilities, the best candidate for this metasomatic agent is an oxidized CO_2-H_2O-rich fluid (Gregory and Taylor 1986; Kempton et al. 1988), perhaps related to the final stages of crystallization of mafic melts traversing the upper mantle (Wilshire 1987; Sen 1988).

We note that oxygen isotope data indicate that minerals in metasomatized xenoliths are not in isotopic equilibrium. Although in a formal sense, this may undermine the use of heterogeneous equilibria to determine fO_2 and temperature in xenolith assemblages. the similarity in temperature based on different thermometers and the close approach to Mg-Fe exchange equilibrium in our final data set suggests that cation chemical equilibrium was closely approached in these xenoliths. As shown in figure 10, moreover, the magnetite content of the spinels is strongly correlated with $\Delta\log fO_2$ (rock-MAA), so even if the quantitative estimates of fO_2 in the metasomatized xenoliths are compromised, the correlation between relative degrees of oxidation

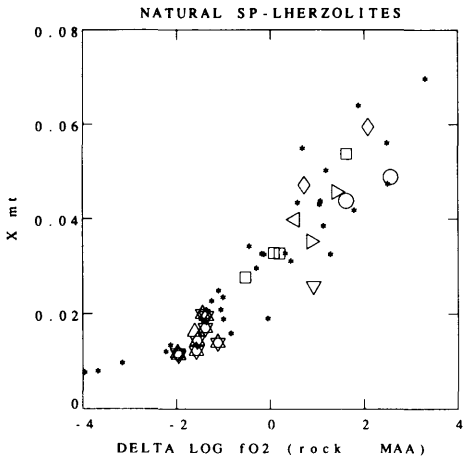

FIG. 10.—X^{sp}_{mt} vs. $\Delta\log_{10}fO_2$ (rock-MAA). There is a good positive correlation between measured Fe^{3+} of the spinel, reflected as X^{sp}_{mt}, and the quantitative measure of fO_2. Symbols are the same as in figure 6.

(as measured by X^{sp}_{mt}) and degree of metasomatism survives.

Relationship of Oxygen Fugacity to Recent and Ancient Subduction.—In the foregoing section, we suggested that oxidation of mantle rocks (leading to positive $\Delta\log fO_2$ (rock-MAA) values) results from interaction with oxidized fluids. Figures 5*a* through 5*e* show that xenoliths from the circumpacific region tend to be more oxidized than the average of the population we have studied. Although oxidizing fluids may be generated in a variety of mantle settings, it is tempting to suggest that subduction and subsequent dehydration of hydrothermally altered oceanic crust and associated sediments generates enriched, oxidized CO_2–H_2O-rich fluids during prograde metamorphism that metasomatize (Gregory and Taylor 1986) and oxidize peridotites in the overlying mantle wedge, and that the oxidized nature of peridotites from the circumpacific results from this process. The most oxidized xenoliths in our data set are from Hawaii and Tahiti (fig. 5*c*). Old oceanic crust has also been suggested to play a role in the genesis of oceanic island basalts (Hofmann and White 1980; Allegre and Turcotte 1985), and their highly oxidized nature could reflect the influence of this subducted material. If subducted material is the source of oxidized fluids in the mantle wedge and in the lithosphere overlying mantle plumes, subduction could have contributed to progressive oxidation of the earth's upper mantle over the entire Phanerozoic, or at least as long as plate tectonics have been active.

CONCLUSIONS

Our calculated fO_2's and temperatures for 280 spinel-bearing lherzolite and harzburgite peridotites define a general trend in fO_2-T space that is not parallel to and has a steeper slope than IW, FMQ, MFF, and MH synthetic Fe buffers. Most calculated fO_2's, however, fall within ± 2 log units of FMQ at 15 kbar. Variations in major-element, trace-element, and oxygen isotopic composition of xenoliths correlate with variations in calculated fO_2. Rare "fertile" xenoliths record fO_2's close to WM buffer at 15 kbar and 900°C. Xenoliths with both cryptic and/or modal metasomatic overprinting are generally oxidized relative to xenoliths without evidence of such open system processing. Based on trace element and oxygen isotopic data, the best candidate for the metasomatic agent is a CO_2–H_2O-rich fluid. Since xenoliths from Hawaii and Tahiti and some from the circumpacific region record fO_2's that are higher than the average of the mantle array, we suggest that some metasomatic fluid could be related to dehydration of downgoing slabs at convergent margins and that this process may have led to progressive oxidation of the earth's upper mantle through much of geologic time.

ACKNOWLEDGMENTS.—G. Mattioli was supported at Caltech as a Dr. Chaim Weizmann Fellow in the Division of Geological and Planetary Sciences during this project. M. Baker and M. Rutter were supported by the NSF by a grant to Prof. P. J. Wyllie (EAR-87-19792). Prof. E. Stolper was supported in part by grants from the NSF (EAR-87-18229) and from NASA (NAG9-105). Division of Geological and Planetary Sciences contribution number 4729. We thank J. D. Pasteris for her review.

REFERENCES CITED

ALBUQUERQUE DE, C. A. R.; CAPEDRI, S.; and DOSTAL, J., 1977, Mineralogy of spinel peridotite inclusions of alkali basalts from Sardinia: Geol. Soc. Amer. Bull., v. 88, p. 1493–1496.

ALLEGRE, C. J., and TURCOTTE, D., 1985, Geody-

namic mixing in the mesosphere boundary layer and the origin of oceanic islands: Geophys. Res. Letters, v. 12, p. 207–210.

AOKI, K., and PRINZ, M., 1974, Chromian spinels in lherzolite inclusions from Itinome-gata, Japan: Contrib. Mineral. Petrol., v. 46, p. 249–256.

———, and SHIBA, I., 1973, Pyroxenes from lherzolite inclusions of Itinome-gata, Japan: Lithos, v. 6, p. 41–51.

———, and ———, 1974, Olivines from lherzolite inclusions of Itinome-gata, Japan: Mem. Geol. Soc. Japan, v. 11, p. 1–10.

ARAI, S., and HIRAI, H., 1983, Petrographical notes on deep-seated and related rocks. (1) Mantle peridotites from Kurose and Nagamadake alkali basalts, southwestern Japan: Ann. Rept. Inst. Geosci. Univ. Tsukaba, v. 9, p. 65–67.

———, and SAEKI, Y., 1980, Ultramafic inclusions from Sannomegata crater, Oga peninsula, Japan, with special reference to the petrological difference from the Itinomegata inclusions: Jour. Geol. Soc. Japan, v. 86, p. 705–708.

ARCULUS, R. J., 1985, Oxidation status of the mantle: past and present: Ann. Rev. Earth Planet. Sci., v. 13, p. 75–95.

———, and DELANO, J., 1981, Intrinsic oxygen fugacity measurements: techniques and results for spinels from upper mantle peridotite and megacryst assemblages: Geochim. Cosmochim. Acta, v. 45, p. 899–913.

———, and ———, 1987, Oxidation state of the upper mantle: present conditions, evolution, and controls, *in* NIXON, P. H., ed., Mantle Xenoliths, Chichester, England, Wiley, p. 119–124.

BASU, A. R., and MACGREGOR, I., 1975, Chromite spinels from ultramafic xenoliths: Geochim. Cosmochim. Acta, v. 89, p. 937–945.

BERMAN, R. G., and BROWN, T., 1985, Heat capacity of minerals in the system Na_2O-FeO-Fe_2O_3-Al_2O_3-SiO_2-TiO_2-H_2O-CO_2: Contrib. Mineral. Petrol., v. 89, p. 168–183.

BOETTCHER, A. L., and O'NEIL, J., 1980, Stable isotope, chemical, and petrographic studies of high-pressure amphiboles and micas: evidence for metasomatism in the mantle source regions of alkali basalts and kimberlites: Am. Jour. Sci., v. 280-A, p. 594–621.

BOHLEN, S. R.; ESSENE, E.; and BOETTCHER, A., 1980, Reinvestigation and application of olivine-quartz-orthopyroxene barometry: Earth Planet. Sci. Letters, v. 47, p. 1–10.

BONATTI, E.; HAMLYN, P.; and OTTONELLO, G., 1981, Upper mantle beneath a young oceanic rift: peridotites from the island of Zabargad (Red Sea): Geology, v. 9, p. 474–479.

BOYNTON, W. V., 1984, Cosmochemistry of the rare earth elements: meteorite studies, *in* HENDERSON, P., ed., Rare Earth Element Geochemistry (Developments in Geochemistry, Vol. 2), Amsterdam, Elsevier, p. 63–114.

BREARLY, M.; SCARFE, C.; and FUJII, T., 1984, The petrology of ultramafic xenoliths from Summit Lake, near Prince George, British Columbia: Contrib. Mineral. Petrol., v. 88, p. 53–63.

BUSSOD, G. Y. A., 1983, Thermal and kinematic history of mantle xenoliths from Kilbourne Hole, New Mexico: Unpub. M.S. thesis, Los Alamos Nat. Lab., Los Alamos, New Mexico, 74 p.

CAO, R.-L., and ZHU, S., 1987, Mantle xenoliths and alkali-rich host rocks in eastern China, *in* NIXON, P. H., ed., Mantle Xenoliths: Chichester, England, Wiley, p. 167–180.

DAUTRIA, J. M., and GIROD, M., 1987, Cenozoic volcanism associated with swells and rifts, *in* NIXON, P. H., ed., Mantle Xenoliths: Chichester, England, Wiley, p. 195–214.

DAVIDSON, P. M., and MUKHOPADHYAY, D., 1984, Ca-Fe-Mg olivines: phase relations and a solution model: Contrib. Mineral. Petrol., v. 86, p. 256–263.

DAWSON, J., 1984, Contrasting types of upper-mantle metasomatism, *in* KORNPROBST, J., ed., Kimberlites-II: The Mantle and Crust-Mantle Relationships (Developments in Petrology, Vol. 11B), Amsterdam, Elsevier, p. 289–294.

DUPUY, C.; DOSTAL, J.; and BODINIER, J., 1987, Geochemistry of spinel peridotite inclusions in basalts from Sardinia: Mineral. Mag., v. 51, p. 561–568.

EGGLER, D. H., and BAKER, D., 1982, Reduced volatiles in the system C-O-H: implications to mantle melting, fluid formation, and diamind genesis, *in* AKIMOTO, S., and MANGHNANI, M., ed., High Pressure Research in Geophysics, Tokyo, Japan, Center for Academic Publications, p. 237–250.

FRANCIS, D., 1987, Mantle-melt interaction recorded in spinel lherzolite xenoliths from the Alligator Lake volcanic complex, Yukon, Canada: Jour. Petrol., v. 28, p. 569–597.

FREY, F. A., 1983, Rare earth element abundances in upper mantle rocks, *in* HENDERSON, P., ed., Rare Earth Element Geochemistry (Developments in Geochemistry, Vol. 2), Amsterdam, Elsevier, p. 153–203.

———, and GREEN, D., 1974, The mineralogy, geochemistry, and origin of lherzolite inclusions in Victorian basanites: Geochim. Cosmochim. Acta, v. 38, p. 1023–1059.

———, and PRINZ, M., 1978, Ultramafic inclusions from San Carlos, Arizona: petrologic and geochemical data bearing on their petrogenesis: Earth Planet. Sci. Lett., v. 38, p. 129–176.

GASPARIK, T., and NEWTON, R., 1984, The reversed alumina contents of orthopyroxene in equilibrium with spinel and forsterite in the system MgO-Al_2O_3-SiO_2: Contrib. Mineral. Petrol., v. 85, p. 186–196.

GIROD, M.; DAUTRIA, J.; and DE GIOVANNI, R., 1981, A first insight into the constitution of the upper mantle under the Hoggar area (southern Algeria): the lherzolite xenoliths in the alkali-basalts: Contrib. Mineral. Petrol., v. 77, p. 66–73.

GREEN, D. H., and RINGWOOD, A., 1967, The genesis of basaltic magmas: Contrib. Mineral. Petrol., v. 15, p. 103–190.

GREGORY, R. T., and TAYLOR, H., JR., 1986, Non-equilibrium, metasomatic $^{18}O/^{16}O$ effects in upper mantle mineral assemblages: Contrib. Mineral. Petrol., v. 93, p. 124–135.

GUTMANN, J. T., 1986, Origin of four- and five-phase ultramafic xenoliths from Sonora, Mexico: Am. Mineral., v. 71, p. 1076–1084.

HAGGERTY, S. E., and TOMPKINS, L., 1983, Redox state of earth's upper mantle from kimberlitic ilmenites: Nature, v. 303, p. 295–300.

HARMON, R. S.; KEMPTON, P.; STOSCH, H.; HOEFS, J.; KOVALENKO, V.; and EONOV, D., 1987, $^{18}O/^{16}O$ ratios in anhydrous spinel lherzolite xenoliths from the Shavaryn-Tsaram volcano, Mongolia: Earth Planet. Sci. Lett., v. 81, p. 193–202.

HART, S. B., and ZINDLER, A., 1986, In search of a bulk-earth composition: Chem. Geol., v. 57, p. 247–267.

HARTE, B., 1983, Mantle peridotites and processes—the kimberlite sample, *in* HAWKESWORTH, C. J., and NORRY, M. J., eds., Continental Basalts and Mantle Xenoliths (Shiva Geology Series): Cheshire, UK, Shiva Publishing, p. 46–91.

HERVIG, R. L., and SMITH, J., 1982, Temperature-dependent distribution of Cr between olivine and pyroxenes in lherzolite xenoliths: Contrib. Mineral. Petrol., v. 81, p. 184–189.

HOFMANN, A. W., and WHITE, W., 1980, The role of subducted oceanic crust in mantle evolution: Carnegie Inst. Washington, Yearbook, v. 79, p. 477–483.

JAGOUTZ, E.; PALME, H.; BADDENHAUSEN, H.; BLUM, K.; CENDALES, M.; DREIBUS, G.; SPETTEL, B.; LORENZ, V.; and WANKE, H., 1979, The abundances of major, minor, and trace elements in the earth's mantle as derived from primitive ultramafic nodules: Proc. Lunar Planet. Sci. Conf., v. 10, p. 2031–2050.

JAQUES, A. L., and GREEN, D., 1980, Anhydrous melting of peridotite at 0–15 kb pressure and the genesis of tholeiitic basalts: Contrib. Mineral. Petrol., v. 73, p. 287–310.

KAWASAKI, T., and MATSUI, Y., 1983, Thermodynamic analyses of equilibria involving olivine, orthopyroxene, and garnet: Geochim. Cosmochim. Acta, v. 47, p. 1661–1679.

KEMPTON, P. D., 1987, Mineralogic and geochemical evidence for differing styles of metasomatism in spinel lherzolite xenoliths: enriched mantle source regions of basalts?, *in* MENZIES, M. A., and HAWKESWORTH, C. J., eds., Mantle Metasomatism: London, Academic Press, p. 45–89.

———; HARMON, R.; STOSCH, H.; HOEFS, J.; and HAWKESWORTH, C., 1988, Open-system O-isotope behavior and trace element enrichment in the sub-Eifel mantle: Earth Planet. Sci. Lett., v. 89, p. 273–287.

KUO, L.-C., and ESSENE, E., 1986, Petrology of spinel harzburgite xenoliths from the Kishb Plateau, Saudi Arabia: Contrib. Mineral. Petrol., v. 93, p. 335–346.

KYSER, T. K.; O'NEIL, J.; and CARMICHAEL, I., 1981, Oxygen isotope thermometry of basic lavas and mantle nodules: Contrib. Mineral. Petrol., v. 77, p. 11–23.

LITTLEJOHN, A. L., and GREENWOOD, H., 1974, Lherzolite nodules in basalts from British Columbia, Canada: Can. Jour. Earth Sci., v. 11, p. 1288–1308.

LLOYD, F. E., and BAILEY, D., 1975, Light element metasomatism of the continental mantle: the evidence and the consequences, *in* AHRENS, L. H., et al., eds., Physics and Chemistry of the Earth, Vol. 9: Oxford, Pergamon Press, p. 389–416.

MATTIOLI, G. S., and WOOD, B., 1986, Upper mantle oxygen fugacity recorded by spinel-lherzolites: Nature, v. 322, p. 626–628.

———, and ———, 1988, Magnetite activities across the $MgAl_2O_4$-Fe_3O_4 spinel join, with application to thermobarometric estimates of upper mantle oxygen fugacity: Contrib. Mineral. Petrol., v. 98, p. 148–162.

———; ———; and CARMICHAEL, I., 1987, Ternary-spinel volumes in the system $MgAl_2O_4$-Fe_3O_4-γ-$Fe_{8/3}O_4$: implications for the effect of P on intrinsic fO_2 measurements of mantle-xenolith spinels: Am. Mineral., v. 72, p. 468–480.

MCGUIRE, A. V., 1988, Petrology of mantle xenoliths from Harrat al Kishb: the mantle beneath western Saudi Arabia: Jour. Petrol., v. 29, p. 73–92.

MEDARIS, L. G., JR., 1972, High-pressure peridotites in southwestern Oregon: Geol. Soc. America Bull., v. 83, p. 41–58.

MEYER, H. O. A., and SVISERO, D., 1987, Mantle xenoliths in South America, *in* NIXON, P. H., ed., Mantle Xenoliths, Chichester, England, Wiley, p. 85–91.

MORRIS, P. A., 1986, Constraints on the origin of mafic alkaline volcanics and included xenoliths from Oberon, New South Wales, Australia: Contrib. Mineral. Petrol., v. 93, p. 207–214.

MORTEN, L., 1987, Italy: a review of xenolithic occurrences and their comparison with Alpine peridotites, *in* NIXON, P. H., ed., Mantle Xenoliths, Chichester, England, Wiley, p. 135–148.

MYERS, J., and EUGSTER, H., 1983, The system Fe-Si-O: oxygen buffer calibrations to 1500 K: Contrib. Mineral. Petrol., v. 82, p. 75–90.

NASIR, S., and AL-FUQHA, H., 1988, Spinel-lherzolite xenoliths from Aritain volcano, NE Jordan: Mineral. Petrol., v. 38, p. 127–137.

NICHOLLS, J.; STOUT, M.; and FIESINGER, D., 1982, Petrologic variations in quaternary volcanic rocks, British Columbia, and the nature of the underlying upper mantle: Contrib. Mineral. Petrol., v. 79, p. 201–218.

O'NEILL, H. ST. C., and WALL, V., 1987, The olivine-orthopyroxene-spinel oxygen geobarometer, the Nickel precipitation curve, and the oxygen fugacity of the earth's upper mantle: Jour. Petrol., v. 28, p. 1169–1191.

OTTONELLO, G., 1980, Rare earth abundances and distribution in some spinel peridotite xenoliths from Assab (Ethiopia): Geochim. Cosmochim. Acta, v. 44, p. 1885–1901.

OZAWA, K., 1988, Ultramafic tectonite of the Miyamori ophiolite complex in the Kitakami Mountains, northeast Japan: hydrous upper mantle in an island arc: Contrib. Mineral. Petrol., v. 99, p. 159–175.

PICCARDO, G. B., and OTTONELLO, G., 1978, Partial melting effects on coexisting minerals compositions in upper mantle xenoliths from Assab (Ethiopia): Rend. Soc. Italia Mineral. Petrol., v. 34, p. 499–526.

PRESS, S.; WITT, G.; SECK, H.; EONOV, D.; and KO-

VALENKO, V., 1986, Spinel peridotite xenoliths from the Tariat Depression, Mongolia I: major element chemistry and mineralogy of a primitive mantle xenolith suite: Geochim. Cosmochim. Acta, v. 50, p. 2587–2599.

REAY, A., and SIPIERA, P., 1987, Mantle xenoliths from the New Zealand region, *in* NIXON, P. H., ed., Mantle Xenoliths, Chichester, England, Wiley, p. 347–358.

ROBIE, R. A.; HEMINGWAY, B.; and FISHER, J., 1978, Thermodynamic properties of minerals and related substances at 298.15 K and 1 bar (10^5 Pascals) pressure and at higher temperatures: Geol. Surv. America Bull., v. 1452, p. 1–456.

RODEN, M. F.; IRVING, A.; and MURTHY, V., 1988, Isotopic and trace element composition of the upper mantle beneath a young continental rift: results from Kilbourne Hole, New Mexico: Geochim. Cosmochim. Acta, v. 52, p. 461–473.

RUTTER, M. J., 1985, Tertiary magmatism in northern Sardinia: Unpub. Ph.D. thesis, Univ. of London, 322 p.

———, 1987, The nature of the lithosphere beneath the Sardinian continental block: mantle and deep crustal inclusions in mafic alkaline lavas: Lithos, v. 20, p. 225–234.

RYABCHIKOV, I. D.; UKHANOV, A.; and ISHII, T., 1986, Redox equilibria in upper mantle ultrabasites in the Yakutia kimberlite province: Geokhimiya Intl., v. 23, p. 38–50.

SACHTLEBEN, TH., and SECK, H., 1981, Chemical control of Al-solubility in orthopyroxene and its implications on pyroxene geothermometry: Contrib. Mineral. Petrol., v. 78, p. 157–165.

SACK, R. O., and GHIORSO, M., 1989, Thermochemistry of minerals in the system Mg_2SiO_4-Fe_2-SiO_4-SiO_2: Contrib. Mineral. Petrol., in press.

SEN, G., 1988, Petrogenesis of spinel lherzolite and pyroxenite suite xenoliths from the Koolan shield, Oahu, Hawaii: implications for petrology of the post-eruptive lithosphere beneath Oahu: Contrib. Mineral. Petrol., v. 100, p. 61–91.

SIAL, A. N., 1977, Petrology and mineral chemistry of peridotite nodules included in Tertiary basaltic rocks of northeast Brazil: Geol. Soc. America Bull., v. 88, p. 1173–1176.

SKEWES, M. A., and STERN, C., 1979, Petrology and geochemistry of alkali basalts and ultramafic inclusions from the Palei-aike volcanic field in southern Chile and the origin of the Patagonian Plateau lavas: Jour. Volcan. Geotherm. Res., v. 6, p. 3–25.

STORMER, J. C.; GOMES, C.; and TORQUANTO, J., 1975, Spinel lherzolite nodules in basanite lavas from Asuncion, Paraguay: Revista Brasil Geosci., v. 5, p. 176–185.

STOSCH, H.-G.; LUGMAIR, G.; and KOVALENKO, V., 1986, Spinel peridotite xenoliths from the Tariat Depression, Mongolia. II: geochemistry and Nd and Sr isotopic composition and their implications for the evolution of the subcontinental lithosphere: Geochim. Cosmochim. Acta, v. 50, p. 2601–2614.

———, and SECK, H., 1980, Geochemistry and mineralogy of two spinel peridotite suites of Dreiser Weiher, West Germany: Geochim. Cosmochim. Acta, v. 44, p. 457–470.

SWANSON, S. E.; KAY, S.; BREARLY, M.; and SCARFE, C., 1987, Arc and back-arc xenoliths in Kurile-Kamchatka and western Alaska, *in* NIXON, P. H., ed., Mantle Xenoliths, Chichester, England, Wiley, p. 304–318.

TAKAHASHI, E., 1980, Thermal history of lherzolite xenoliths I. Petrology of lherzolite xenoliths from the Ichinomegata crater, Oga peninsula, northeast Japan: Geochim. Cosmochim. Acta, v. 44, p. 1643–1658.

———, 1986, Melting of a dry peridotite KLB-1 up to 14 GPa: implications on the origin of peridotitic upper mantle: Jour. Geophys. Res., v. 91, p. 9367–9382.

TRACY, R. J., 1980, Petrology and genetic significance of an ultramafic xenolith suite from Tahiti: Earth Planet. Sci. Lett., v. 48, p. 80–96.

ULMER, G. C.; GRANDSTAFF, D.; WEISS, D.; MOATS, M.; BUNTIN, T.; GOLD, D.; HATTON, C.; KADIK, A.; KOSELUK, R.; and ROSENHAUER, M., 1987, The mantle redox state; an unfinished story?, *in* MORRIS, E. M., and PASTERIS, J. D., eds., Mantle metasomatism and alkaline magmatism: Geol. Soc. America Spec. Paper 215, p. 5–23.

VARNE, R., 1977, On the origin of spinel lherzolite inclusions in basaltic rocks from Tasmania and elsewhere: Jour. Petrol., v. 18, p. 1–23.

VIRGO, D. A.; LUTH, R.; MOATS, M.; and ULMER, G., 1988, Constraints on the oxidation state of the mantle: an electrochemical and ^{57}Fe Mossbauer study of mantle-derived ilmenites: Geochim. Cosmochim. Acta, v. 52, p. 1781–1794.

WEBB, S. A. CARROLL, and WOOD, B., 1986, Spinel-pyroxene-garnet relationships and their dependence on Cr/Al ratio: Contrib. Mineral. Petrol., v. 92, p. 471–480.

WELLS, P. R. A., 1977, Pyroxene thermometry in simple and complex systems: Contrib. Mineral. Petrol., v. 62, p. 129–139.

WILSHIRE, H. G., 1987, A model of mantle metasomatism, *in* MORRIS, E. M., and PASTERIS, J. D., eds., Mantle metasomatism and alkaline magmatism: Geol. Soc. America Spec. Paper 215, p. 47–59.

———, and SHERVIS, J., 1975, Al-augite and Cr-diopside ultramafic xenoliths in basaltic rocks from western United States, *in* AHRENS, L. H., et al., eds., Physics and Chemistry of the Earth, Vol. 9, Oxford, Pergamon Press, p. 257–272.

WOERMANN, E., and ROSENHAUER, M., 1985, Fluid phases and the redox state of the earth's mantle: extrapolations based on experimental, phase-theoretical and petrological data: Fortsch. Miner., v. 63, p. 263–349.

WOOD, B. J., and BANNO, S., 1973, Garnet-orthopyroxene and orthopyroxene-clinopyroxene relationships in simple and complex systems: Contrib. Mineral. Petrol., v. 42, p. 109–124.

———, and YUEN, D., 1983, The role of lithospheric phase transitions on seafloor flattening at old ages: Earth Planet. Sci. Lett., v. 66, p. 303–314.